# Spin splitting of X-valley-related donor impurity states in an AlAs barrier

E. E. Vdovin,[1] Yu. N. Khanin,[1] L. Eaves,[2] M. Henini,[2] and G. Hill[3]
[1]*Institute of Microelectronics Technology and High Purity Material, Russian Academy of Sciences, Chernogolovka, Moscow District, 142432 Russia*
[2]*School of Physics and Astronomy, University of Nottingham, Nottingham, NG7 2RD, United Kingdom*
[3]*Department of Electronic and Electrical Engineering, University of Sheffield, Sheffield, S3 3JD, United Kingdom*
(Received 20 August 2004; revised manuscript received 30 November 2004; published 23 May 2005)

We use magnetotunneling spectroscopy to observe the spin splitting of the ground state of an X-valley-related Si-donor impurity in an AlAs barrier. We determine the absolute magnitude of the effective Zeeman spin splitting factors of the impurity ground state to be $g_I = 2.2 \pm 0.1$. We also investigate the spatial form of the electron wave function of the donor ground state, which is anisotropic in the growth plane.

DOI: 10.1103/PhysRevB.71.195320 PACS number(s): 73.40.Gk, 71.70.Ej, 71.55.Eq

## I. INTRODUCTION

The effect of spin on electronic transport has recently attracted much interest both from an applied and from a fundamental point of view.[1,2] Resonant electron tunneling through the discrete states of self-assembled semiconductor quantum dots (QD's) and the physically similar bound states of impurities is a promising means of studying spin-resolved transport. Such tunneling experiments have been used to observe directly the spin splitting of the bound electronic states of shallow impurities within a GaAs quantum well[3–5] or of electrons in InAs QD's (Refs. 6–8) and to measure directly the absolute value of the $g$ factor of these zero-dimensional states. In addition, they have been used to probe at a mesoscopic level the spin dependence of the local density of states.[9] Resonant tunneling studies have also been performed on single-barrier GaAs/AlAs/GaAs heterostructures. AlAs is an indirect-gap material with the minima of the conduction band at the X points of the Brillouin zone, whereas in GaAs the minimum is at the $\Gamma$ point. There have been several earlier studies of tunneling through X-valley states,[10–16] including investigations of the tunneling through donor states associated with the X- conduction-band minima.[17–23]

In this paper, we report the observation of Zeeman spin splitting of the ground state of an Si-donor impurity embedded in an AlAs tunnel barrier for the orientation in which the magnetic field is applied in the plane of the barrier—i.e., perpendicular to the direction of the electron tunnel current. This state is associated with the anisotropic X-conduction-band minima of AlAs. The Si atoms, which are located substitutionally on Al sites, diffuse during growth into the AlAs barrier from adjacent GaAs layers which are $\delta$ doped with Si. We measure the effective $g$ factor of the zero-dimensional state and obtain the absolute values of the effective spin-splitting factor components $g$ of between 2.1 and 2.2. In addition, magnetotunneling spectroscopy provides us with information about the spatial form of the wave function of an electron bound in the X-valley-related donor state. Our measurements indicate that the wave function has a biaxial symmetry in the growth plane, with axes corresponding to the main crystallographic directions of the (001) epilayers.

Let us first briefly review the previously studied problem of tunneling through isolated donor impurities in the GaAs quantum well (QW) of large-area GaAs/(AlGa)As double-barrier resonant tunneling diodes. In this case the donors form localized ($\sim$10 nm) hydrogenic bound states associated with the $\Gamma$-conduction-band minimum of the GaAs QW.[24] These states are located at an energy of $\sim$10 meV below the bottom of the lowest-energy subband of the QW. Under an applied bias the tunnel current exhibits a rapid increase when the impurity state aligns with the Fermi level in the negatively biased electron emitter layer. In general, there are many impurities giving rise to multiple, overlapping steps in the current-voltage characteristics, and these multiple peaks can be resolved in the current-voltage characteristics of small-area mesa samples.[22] Similarly, in our previous work, the resonant tunneling of electrons through individual X-valley-related donor impurity states of a single, relatively thin, 5-nm AlAs barrier (with an X-conduction-band quantum well) appeared as partially resolved fine structure in a broad resonance, associated with the ensemble of donors.[21] This fine structure arises because the donors are located in different atomic planes of the AlAs and the spectrum of donor states is determined predominantly by the dependence of the binding energy on the position of the donor in the barrier. The influence of the random variations of the electrostatic potential on the energies of the donor impurity in this case is insignificant.

In contrast, for the experiments described here, the donors are randomly located in a relatively thick, 11.2-nm, barrier, so the influence of the random electrostatic potential is considerable. The essential role of the random variations of the electrostatic potential in this case is associated with the presence of the $\delta$-doped layers near the barrier[25] and the slow dependence of the binding energy of donors on their position in the thick barrier.[26] As a result, resonant tunneling of electrons through the donor states gives rise to a series of sharp, well-resolved peaks in the $I(V)$ curves. We ascribe each peak to tunneling through a single or very small number of individual donor states. This allows us to observe spin splitting of the donor resonances and to determine the $g$ factor of the zero-dimensional states directly.

## II. SAMPLES

A schematic diagram of our device is shown in Fig. 1. The active part of our samples comprises a single 11.2-nm-thick

 ©2005 The American Physical Society

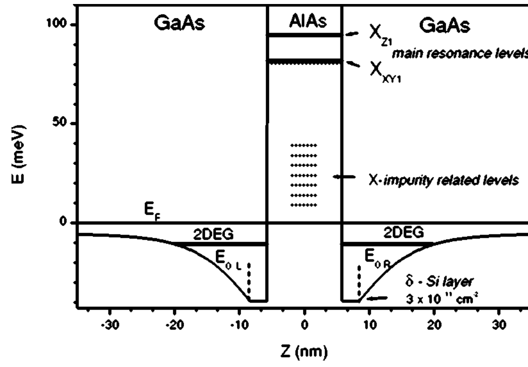


FIG. 1. Calculated conduction band profile of the active part of the tunnel structure at zero applied voltage. The figure shows the positions of the Fermi level $E_F$, the quantized GaAs accumulation layer subbands $E_{0L}$ and $E_{0R}$, and the size-quantized levels of the $X_Z$ and $X_{XY}$ subbands in the AlAs barrier. The energy positions of the X-impurity-related levels in AlAs are also shown.

AlAs barrier which is sandwiched between two accumulation layers formed by two $\delta$-doped layers with Si concentration of $3\times10^{11}$ cm$^{-2}$, located at a distance of 2.8 nm from each side of the barrier. A two-dimensional electron gas (2DEG) forms in each accumulation layer at zero bias. The AlAs layer was not intentionally doped, but donor impurities are present in the AlAs due to diffusion of Si into the barrier from the $\delta$-doped layers. The calculated $\Gamma$- and X-band profiles of the active part of our device at zero bias are shown in Fig. 1. The heterostructure was grown by molecular beam epitaxy on a (001)-oriented, Si-doped $n^+$-type GaAs wafer ($N_d=2\times10^{18}$ cm$^{-3}$) at a temperature of 550 °C. The detailed layer composition of the heterostructure, in order of growth on the substrate, is as follows: a Si-doped, 0.5-$\mu$m-thick GaAs buffer layer ($N_d=2\times10^{18}$ cm$^{-3}$), a 60-nm-thick GaAs layer ($N_d=3\times10^{17}$ cm$^{-3}$), a 21.6-nm-thick undoped GaAs layer; a 5.6-nm-thick undoped $Ga_{0.9}Al_{0.1}As$ layer, a 28-nm-thick undoped GaAs layer, a Si $\delta$-doped layer with concentration of $3\times10^{11}$ cm$^{-2}$, a 2.8-nm-thick undoped GaAs layer, a 11.2-nm-thick AlAs barrier layer; a 2.8-nm-thick undoped GaAs layer, a Si $\delta$-doped layer with concentration of $3\times10^{11}$ cm$^{-2}$, a 28-nm-thick undoped GaAs layer, 5.6-nm-thick undoped $Ga_{0.9}Al_{0.1}As$ layer, a 21.6-nm-thick undoped GaAs layer, a 60-nm-thick GaAs layer ($N_d=3\times10^{17}$ cm$^{-3}$), and a 0.5-$\mu$m-thick, GaAs cap layer ($N_d=2\times10^{18}$ cm$^{-3}$). Ohmic contacts were made by deposition and annealing of AuGe/Ni/Au layers. Mesa structures, with a diameter between 50 $\mu$m and 200 $\mu$m, were fabricated by chemical etching.

## III. EXPERIMENT

Tunnel current measurements at constant applied voltage with magnetic field $B$ applied parallel to the current (i.e., perpendicular to the 2DEG) reveal Shubnikov–de Haas–(SdH-) like oscillations.[27] Close to zero applied bias, analysis of the SdH-like oscillations gives a value of $n_s=3.27\times10^{11}$ cm$^{-2}$ for the sheet density of the two 2DEG layers. Figure 2(b) shows the low-temperature (4.2-K) current-

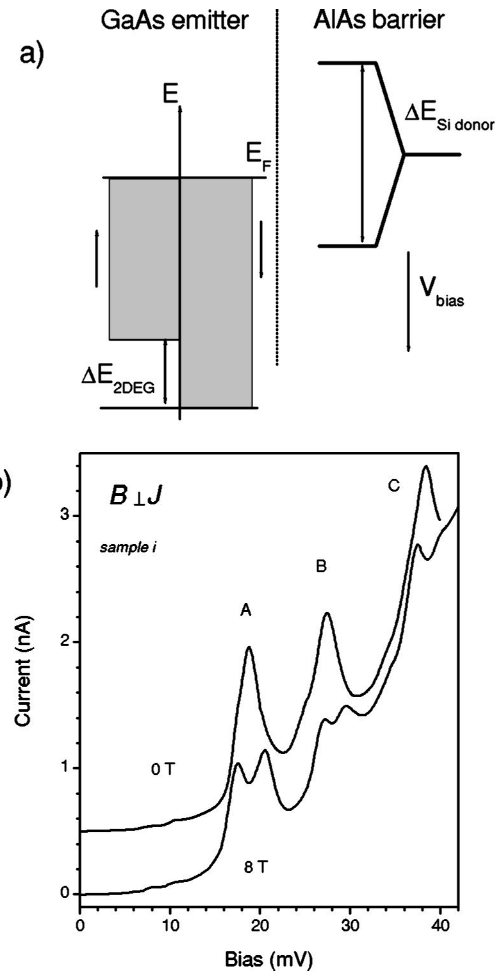


FIG. 2. (a) Schematic diagram of the spin splitting of the Si donor state in the AlAs and partial spin polarization of the 2DEG in a magnetic field applied perpendicular to the current. The effect of applying a voltage across the device is to move the energy donor energy levels down relative to the Fermi level of the 2DEG. (b) $I(V)$ characteristics at 4.2 K of sample $i$ at 0 T and 8 T for a magnetic field applied perpendicular to the current. The curves are offset for clarity. The characteristics show sharp peaks in the current due to tunneling through discrete X-impurity states, each of which split in an applied magnetic field.

voltage $I(V)$ characteristics at low bias voltages for a typical device $i$, which exhibit sharp peaks in the current over voltage range from 10 to 60 mV. This peak structure is observed to be sample specific, but for a given sample it is exactly reproducible from one voltage sweep to another. The peaks are reproducible even after thermal cycling of the sample, except for a small voltage shift (~ a few mV). We ascribe the peaks in current to single-electron tunneling through individual, zero-dimensional Si-donor states in the AlAs barrier. Similar features have been observed and reported previously in large-area double-barrier room-temperature devices (RTD's) (Refs. 3, 5, and 28) and attributed to tunneling through individual tunneling channels due to zero-dimensional states. Increasing the voltage across the device moves the energy of the donor state relative to the Fermi level of the 2DEG that acts as an emitter for the tunneling

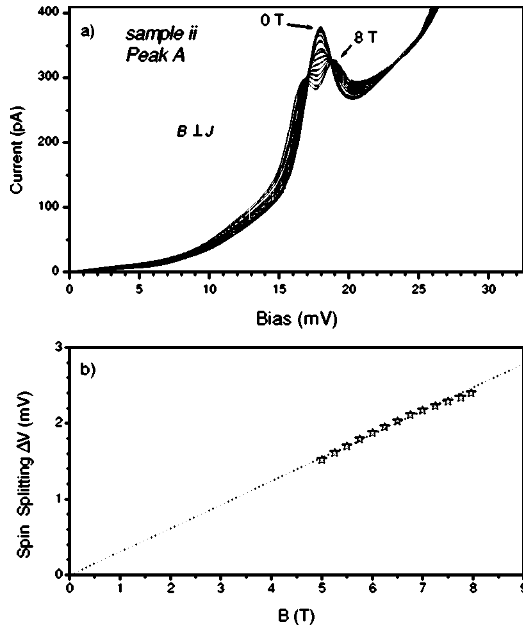


FIG. 3. (a) Evolution of the spin-split peaks in $I(V)$ of the sample *ii* at 4.2 K in various magnetic fields perpendicular to the current from $B=0$ T to 8 T, in steps of 0.5 T. (b) The measured spin splitting versus magnetic field. The dashed lines are linear fits to the data.

electrons [Fig. 2(a)]. Tunneling occurs as the donor state crosses the Fermi level of the 2DEG and stops when the donor state is brought below the 2DEG subband edge.

Figure 2 shows $I(V)$ at 0 and 8 T with magnetic field oriented perpendicular to the current direction. In a magnetic field the ground state of an Si-donor impurity splits into two spin energy levels given by

$$E_{\mathrm{Si}} = g_I \mu_B B m_s (m_s = \pm 1/2), \qquad (1)$$

where $g_I$ is the $g$ factor of the Si-donor impurity. This opens up two separate channels for electrons from the 2DEG to tunnel into, and we therefore see separate peaks in $I(V)$ due to electrons tunneling through each of these spin energy levels. In a magnetic field applied perpendicular to the current (i.e., parallel to the 2DEG) the 2DEG emitter becomes partially spin polarized, due to energy splitting of the Fermi energies of the two spin species, as shown schematically in Fig. 2(a). Due to the slow tunneling rate from the 2DEG, the two spin species in the 2DEG should be in thermal equilibrium, and so the chemical potential of each is the same. Therefore, there is an energy difference between the subband edge of the spin species, equal to the spin splitting $g_{2D}\mu_B B$, where $g_{2D}$ is the $g$ factor of electrons in the 2DEG emitter. Resonant tunneling occurs when an impurity spin level crosses the Fermi level of the 2DEG. We assume that spin is conserved during the tunneling process. For each spin we see a separate onset of tunneling and the voltage difference between the position of the onsets ($\Delta V_{peak}$) is proportional to the energy difference $\Delta E_{\mathrm{Si}} = g_I \mu_B B$ obtained from Eq. (1).

Figure 3(a) shows in detail the behavior of the first current peak of device *ii* at 4.2 K in different magnetic fields applied

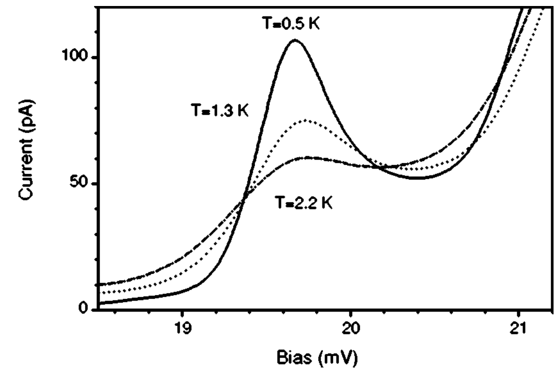


FIG. 4. $I(V)$ characteristics of the first current peak of the typical samples at different temperatures showing the Fermi-level broadening.

perpendicular to the current direction from $B=0$ T to 8 T, in steps of 0.5 T. Figure 3(b) shows the voltage separation between the corresponding two spin-split peaks, which increases linearly with magnetic field strength as expected for a Zeeman effect. Because of the finite widths of the current peaks, it is not possible to resolve the splitting for magnetic fields less than 5 T. The best fit line to the data closely intersects $\Delta V=0$ at $B=0$ T and has a slope $g_I \mu_B / f$, where $\mu_B$ is the Bohr magneton, $g_I$ is the effective gyromagnetic ratio of the impurity with the magnetic field perpendicular to the current (i.e., perpendicular to the growth direction of the quantum well), and $f$ is the so-called electrostatic leverage factor. The temperature dependence of the current onset allows us to determine the electrostatic leverage factor $f$.[4,6] Figure 4 shows the temperature dependence of the onset of a typical resonant current features. We deduce a value of 0.44 for the electrostatic leverage factor by fitting the Fermi-Dirac function to the form of the measured low bias onset of the peak in current at various temperatures, using the procedure described in Ref. 6. A similar value of $f$ is obtained from self-consistent Poisson-Schrödinger calculations: these indicate that, over the bias range of interest (0–100 mV), the leverage factor $f$ for an electron tunneling from the emitter into an impurity located at the center of AlAs barrier varies slightly from 0.44 to 0.42 eV per volt of applied bias. The uncertainty in our value of $g$ is determined by the error in the leverage factor. Note also from Fig. 4 that the resonant peak in $I(V)$ is strongly enhanced as the temperature is reduced. The enhancement, which may be related to a many-body Fermi energy singularity effect,[29] tends to improve the resolution of the spin-split peaks.

We have measured the splitting of several peaks in $I(V)$ and find that the different impurity-related peaks give values of $g_I$ in the range from 2.1 to 2.22. Our value of the $g$ factor of the X-valley-related impurity states in AlAs is of a larger absolute value than reported in another tunneling experiment,[20] where $g=0.34$. However, for the experiment described here, the donors are located in a relatively thick, 11.2-nm, AlAs layer, whereas the localized state investigated in Ref. 20 was embedded in a narrow 2-nm AlAs barrier. This value of $g=0.34$ is quite different from that for the X-valley electrons in bulk AlAs. The $g$ factor for electrons in bulk AlAs expected from theoretical calculations is 1.9,[30]

and the $g$ factor of electrons in bulk $Al_{0.8}Ga_{0.2}As$ has been measured by electron paramagnetic resonance to be 1.96.[31] Also, van Kesteren *et al.* have reported a value of $\approx 1.97$ for electrons in AlAs QW's based on optically detected magnetic resonance experiments on AlAs-GaAs superlattices.[32] This difference in values may be due to the complex nature of the X-valley-related donor impurity states in the AlAs barrier.[20] In low-dimensional heterostructures, it is known that the value of the $g$ factor can be modified from its bulk value, due to quantum confinement effects and because the electron wave function contains contributions from the different materials which make up the structure.[4,33,34] Calculations show that $g$ is a strong function of the quantum well width,[35] and the rather wide X-minimum quantum well of our AlAs barrier gives a $g$ factor of the X donor in our experiment that is close to the $g$ value of bulk AlAs, $g \approx 2$, since the modification of the band structure due to the quantum confinement is fairly small.

We also studied the $g$-factor dependence for a magnetic field applied along different crystallographic axes in the (001) growth plane. In contrast to the case of single-electron tunneling through the localized states of InAs quantum dots,[8] to within the resolution of our experiment, the spin splitting of the X-valley-related donor impurity in AlAs was isotropic with respect to the angle of the in-plane magnetic field.

We now consider the magnetic field dependence of the amplitude of the tunnel current through the X-valley-related donor impurities as a function of magnetic field $B$ applied perpendicular to the direction of tunneling. We attribute the general fall in amplitude of both spin-split components with increasing $B$ [see Fig. 5(a)] to a well-established effect that can be understood in term of a single-particle model for electron tunneling in the presence of a magnetic field.[24,36,37] Let $\alpha$, $\beta$, and $Z$ indicate, respectively, the direction of $B$, the direction normal to $B$ in the growth plane $(X,Y)$, and the normal to the tunnel barrier, respectively. When an electron tunnels from the emitter accumulation layer into the impurity state in the barrier, it acquires an additional in-plane momentum given by

$$k_\beta = eB\Delta s/\hbar, \tag{2}$$

where $\Delta s$ is the effective distance tunneled along $Z$ ($\sim 8$ nm for our device). This gives an increased momentum along $\beta$, which is acquired by the tunneling electron due to the action of the Lorentz force.

The applied voltage allows us to tune resonantly to the energy of a particular impurity state. Thus, by measuring the variation of the tunnel current with $B$, we can determine the size of the matrix element that governs the quantum transition of an electron as it tunnels from a state in the emitter layer into an impurity state.

In order to analyze the results of our experiment, we express the tunneling matrix element $M$ in terms of the Fourier transforms $\Phi_{i(f)}(k)$ of the conventional real-space wave functions, according to the relation $M = \int_k \Phi_i(k-k_\beta)\Phi_f(k)dk$, and express the tunneling current as $I \sim |M|^2$.[24,37] Here the subscripts $i$ and $f$ indicate the initial (emitter) and final (Si-impurity) states of the tunnel transition. Relative to the strong spatial confinement in the zero-dimensional impurity

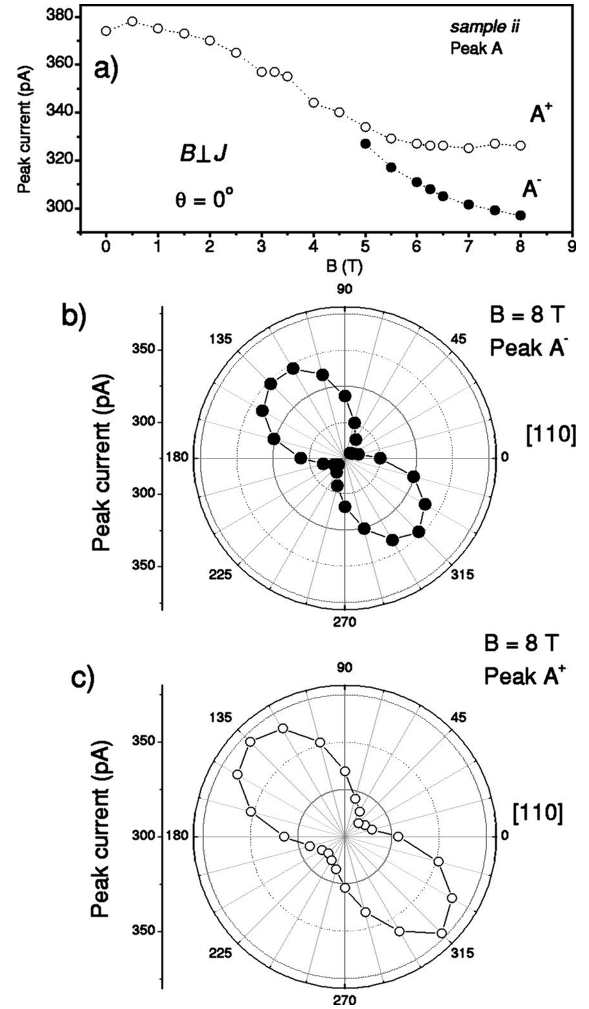


FIG. 5. (a) Amplitude dependence of the peak $A$ of sample *ii* vs magnetic field $\boldsymbol{B}$ applied parallel to a [110] direction in the plane of the quantum well. Polar plot of the change in peak current vs in-plane magnetic field direction for the peaks $A+$ (b) and $A-$ (c) at 8 T.

state, the initial state in the emitter is essentially unconfined—i.e., it behaves like a free particle. Hence, in $k$ space $\Phi_i(k)$ corresponds to a sharply peaked function with a finite value only close to $k=0$. Since the tunnel current is given by the square of the matrix element involving $\Phi_i(k)$ and the Fourier transform of the Si-donor wave function $\Phi_{Si}(k)$, the narrow spread of $k$ for $\Phi_i(k)$ allows us to investigate the form of $\Phi_{Si}(k)$ by varying $B$ and hence $k$, according to Eq. (2). Thus by plotting $I(B)$ for a *particular* direction of $B$ we can measure the dependence of $|\Phi_{Si}(k)|^2$ along the $k$ direction perpendicular to $B$. Then, by rotating $B$ in the plane $(X,Y)$ and making a series of measurements of $I(B)$ with $B$ set at regular intervals ($\Delta\theta \sim 15°$) of the rotation angle $\theta$, we obtain a full spatial profile of $|\Phi_{Si}(k_X,k_Y)|^2$. This represents the projection in $k$ space of the probability density of a given impurity electronic state peak.

Typical experimental data for sample *ii*, of the variation of the current at peak $A$ with the direction of magnetic field at 8 T, are shown as polar plots in Figs. 5(b) and 5(c). A maximum current modulation $\Delta I/I$ of about $\sim 23\%$ is ob-

served, with clear, twofold anisotropy observed for the two split peaks $A^-$ and $A^+$. The anisotropy of each of the observed peaks has a similar magnitude and orientation. In Fig. 5, 0° corresponds to the [110] direction, so the principal axes for the anisotropy are oriented along the [100] and [010] directions. This result shows that the wave-function shape of the X-valley-related donor impurity in AlAs barrier is anisotropic in the growth plane, with the wave-function probability density elongated along the direction [100] in real space. This is in contrast to the case of Si donor states in a GaAs quantum well, where the electron wave function has circular symmetry in the growth plane, as expected for a 1*s* donor ground state.[37] We suggest that this anisotropy may be related to the anisotropy of the effective mass of the electrons in the X-conduction-band minima of AlAs, though this point requires further theoretical analysis.

In conclusion, we have used magnetotunneling spectroscopy to observe the spin splitting of the ground state of Si donor impurities in an AlAs tunnel barrier. These states are associated with the X-conduction-band minima of AlAs. We determine the absolute magnitude of the anisotropic effective magnetic spin-splitting factors $g$ for these states to be $2.1 \pm 0.1$. In addition, we use magnetotunneling spectroscopy to investigate the spatial form of the wave function of the X-valley-related donor impurity. The wave function of electrons bound to an X-related donor has a biaxial symmetry in the growth plane, with axes corresponding to the main crystallographic directions.

## ACKNOWLEDGMENTS

The work is partly supported by RFBR (03-02-17693) and EPSRC (UK). E.E.V. gratefully acknowledges support from the Royal Society. The authors thank Y.V. Dubrovskii and K.A. Benedict for useful discussions, and V. V. Belov for technical assistance.

[1] D. Loss and D. P. DiVincenzo, Phys. Rev. A **57**, 120 (1998).
[2] R. Hanson, B. Witkamp, L. M. K. Vandersypen, L. H. Willems van Beveren, J. M. Elzerman, and L. P. Kouwenhoven, Phys. Rev. Lett. **91**, 196802 (2003).
[3] J. W. Sakai, N. La Scala, Jr., P. C. Main, P. H. Beton, T. J. Foster, A. K. Geim, L. Eaves, M. Henini, G. Hill, and M. A. Pate, Solid-State Electron. **37**, 965 (1994).
[4] M. R. Deshpande, J. W. Sleight, M. A. Reed, R. G. Wheeler, and R. J. Matyi, Phys. Rev. Lett. **76**, 1328 (1996).
[5] J. Köneman, P. Konig, and R. J. Haug, Physica E (Amsterdam) **13**, 675 (2002).
[6] A. S. G. Thornton, T. Ihn, P. C. Main, L. Eaves, and M. Henini, Appl. Phys. Lett. **73**, 354 (1998).
[7] I. Hapke-Wurst, U. Zeitler, H. Frahm, A. G. M. Jansen, R. J. Haug, and K. Pierz, Phys. Rev. B **62**, 12 621 (2000).
[8] I. Hapke-Wurst, U. Zeitler, R. J. Haug, and K. Pierz, Physica E (Amsterdam) **13**, 802 (2002).
[9] P. König, T. Schmidt, and R. J. Haug, Europhys. Lett. **54**, 495 (2001).
[10] E. E. Mendez, W. I. Wang, E. Calleja, and C. E. T. Goncalves da Silva, Appl. Phys. Lett. **50**, 1263 (1987).
[11] Y. Carbonneau, J. Beerens, L. A. Cury, H. C. Liu, and M. Burchanan, Appl. Phys. Lett. **62**, 1955 (1993).
[12] J. J. Finley, R. J. Teissier, M. S. Skolnick, J. W. Cockburn, R. Grey, G. Hill, and M. A. Pate, Phys. Rev. B **54**, R5251 (1996).
[13] R. Teissier, J. J. Finley, M. S. Skolnick, J. W. Cockburn, J.-L. Pelouard, R. Grey, G. Hill, M. A. Pate, and R. Planel, Phys. Rev. B **54**, R8329 (1996).
[14] J. M. Smith, P. C. Klipstein, R. Grey, and G. Hill, Phys. Rev. B **58**, 4708 (1998).
[15] H. Im, P. C. Klipstein, R. Grey, and G. Hill, Phys. Rev. Lett. **83**, 3693 (1999).
[16] H. Im, P. C. Klipstein, R. Grey, and G. Hill, Phys. Rev. B **62**, 11 076 (2000).
[17] H. Fukuyama and T. Waho, Jpn. J. Appl. Phys., Part 2 **34**, L342 (1995).
[18] Yu. N. Khanin, E. E. Vdovin, K. S. Novoselov, Y. Dubrovskii, P. Omling, and S.-B. Carlsson, Jpn. J. Appl. Phys., Part 1 **37**, 3245 (1998).
[19] I. E. Itskevich, L. Eaves, P. C. Main, M. Henini, and G. Hill, Phys. Rev. B **57**, 7214 (1998).
[20] S. A. Vitusevich, A. Forster, K. M. Indlekofer, H. Luth, A. E. Belyaev, B. A. Glavin, and R. V. Konakova, Phys. Rev. B **61**, 10 898 (2000).
[21] Yu. N. Khanin, E. E. Vdovin, Yu. V. Dubrovskii, K. S. Novoselov, S.-B. Carlsson, and P. Omling, Phys. Rev. B **66**, 073302 (2002).
[22] M. Gryglas, M. Baj, B. Chenaud, B. Jouault, A. Cavanna, and G. Faini, Phys. Rev. B **69**, 165302 (2004).
[23] Yu. N. Khanin, E. E. Vdovin, and Yu. V. Dubrovskii, Semiconductors **38**, 419 (2004).
[24] J. W. Sakai, T. M. Fromhold, P. H. Beton, L. Eaves, M. Henini, P. C. Main, F. W. Sheard, and G. Hill, Phys. Rev. B **48**, 5664 (1993).
[25] P. McDonnell, T. J. Foster, P. C. Main, L. Eaves, N. Mori, J. W. Sakai, M. Henini, and G. Hill, Semiconductors **40**, 409 (1996).
[26] G. Weber, Appl. Phys. Lett. **67**, 1447 (1995).
[27] K. S. Chan, F. W. Sheard, G. A. Toombs, and L. Eaves, Phys. Rev. B **56**, 1447 (1997).
[28] J. W. Sakai, P. C. Main, P. H. Beton, N. La Skala, Jr., A. K. Geim, L. Eaves, and M. Henini, Appl. Phys. Lett. **64**, 2563 (1994).
[29] A. K. Geim, P. C. Main, N. La Scala, Jr., L. Eaves, T. J. Foster, P. H. Beton, J. W. Sakai, F. W. Sheard, M. Henini, G. Hill, and M. A. Pate, Phys. Rev. Lett. **72**, 2061 (1994).
[30] L. M. Roth, B. Lax, and S. Zwerdling, Phys. Rev. **114**, 90 (1959).
[31] R. Bottcher *et al.*, Phys. Status Solidi B **58**, K23 (1973).
[32] H. W. van Kesteren, E. C. Cosman, W. A. J. A. van der Poel, and C. T. Foxon, Phys. Rev. B **41**, 5283 (1990).
[33] M. J. Snelling, G. P. Flinn, A. S. Plaut, R. T. Harley, A. C. Tropper, R. Eccleston, and C. C. Phillips, Phys. Rev. B **44**, 11 345 (1991).
[34] E. L. Ivchenko and A. A. Kiselev, Sov. Phys. Semicond. **26**, 827 (1992).
[35] A. A. Kiselev, E. L. Ivchenko, and U. Rossler, Phys. Rev. B **58**,

16353 (1998).
[36] E. E. Vdovin, A. Levin, A. Patane, L. Eaves, P. C. Main, Yu. N. Khanin, Yu. V. Dubrovskii, M. Henini, and G. Hill, Science **290**, 122 (2000).
[37] A. Patane, R. J. A. Hill, L. Eaves, P. C. Main, M. Henini, M. L. Zambrano, A. Levin, N. Mori, C. Hamaguchi, Yu. V. Dubrovskii, E. E. Vdovin, D. G. Austing, S. Tarucha, and G. Hill, Phys. Rev. B **65**, 165308 (2002).